Available online at www.sciencedirect.com

SCIENCE DIRECT®

Journal of Photochemistry and Photobiology A: Chemistry 160 (2003) 77–85

Journal of Photochemistry and Photobiology A:Chemistry

www.elsevier.com/locate/jphotochem

Controlled mass transport as a means for obtaining selective photocatalysis

Sudeshna Ghosh-Mukerji, Hossam Haick, Yaron Paz*

Department of Chemical Engineering, The Water Research Institute and The Institute of Catalysis, Technion, Haifa 32000, Israel

Received 9 January 2003; received in revised form 8 February 2003; accepted 10 April 2003

Abstract

The photoinduced degradation of pollutants in water and air using titanium dioxide attracts an increasing attention. Unfortunately, titanium dioxide has very poor selectivity and cannot differentiate between highly hazardous contaminants that are often non-biodegradable and contaminants of low toxicity that are often very easy to handle biologically. A new approach for enhancing the photocatalytic degradation of specific contaminants in air or water is presented herein. The method is based upon selective physisorption of the contaminants on molecular recognition sites located in the vicinity of titanium dioxide micro-domains, followed by surface-diffusion of the contaminants to the photocatalytic sites. The feasibility of this approach is demonstrated using β-cyclodextrin as the host and 2-methyl-1,4-naphthoquinone and the dye-stuff Chicago Blue as guests. A degradation rate increase of 200 and 70% relative to samples that did not contain the molecular recognition sites was found for the former contaminant and for the latter contaminant, respectively. This was achieved without any significant damage to the organic molecular recognition sites, thus encouraging attempts to materialize this approach on a practical level.

Keywords: Photocatalysis; Titanium dioxide; Cyclodextrin; Surface-diffusion

1. Introduction

Heterogeneous photocatalysis, using titanium dioxide as the photocatalyst of choice, is a useful technique for the degradation of many contaminants in air, in water or on solid surfaces [1]. The general scheme for the photocatalytic destruction of organic compounds involves the excitation of this semiconductor by irradiation with suprabandgap photons and migration of the electron–hole pairs to the surface of the photocatalyst, where the holes may be trapped by H_2O or OH^- adsorbed at the surface, thus forming highly reactive hydroxyl radicals. Since oxidation is governed by a free radical mechanism, it is expected to operate in a non-selective manner. Indeed, it was found [2] that the degradation rate of a large variety of molecules is approximately the same, provided that these molecules adsorb on the photocatalyst's surface. This lack of sensitivity to the type of contaminants seems to be benevolent at first glance. However, poor selectivity also implies that the photocatalyst does not differentiate between highly hazardous contaminants and organic contaminants of low toxicity. This shortcoming is farther aggravated by the fact that while many low toxicity contaminants can be degraded by biological means, many of the highly hazardous materials are non-biodegradable. To this one may add the fact that the adsorption coefficient of many of the chlorinated xenobiotic compounds on titanium dioxide surface is very low, due to their hydrophobic nature.

Selectivity can be enhanced by manipulating the adsorption of the contaminants on the photocatalyst's surface. One way to achieve it is by controlling the surface's electric charge [3,4]. The isoelectric point of titanium dioxide is approximately at pH 6, hence pH values higher than 6 are favorable for the adsorption of positively charged contaminants, while pH values lower than 6 are favorable for the adsorption of negatively charged contaminants. In that manner, the pH dependence of the mineralization rate during the photodegradation of methanol was explained by the adsorption of the intermediate product formic acid [5]. Although performing the photocatalytic process at a predetermined pH helps to differentiate between positively charged contaminants and negatively charged contaminants, the pH effect is not sufficient to obtain high selectivity due to its lack of specificity and due to the fact that most contaminants are neutral.

Enhanced photocatalytic degradation of molecules may be achieved by promoting the adsorption of specific contaminants. Recently, arginine-modified titanium dioxide particles were used to enhance the degradation of nitrobenzene

---

* Corresponding author. Tel.: +972-4-829-2486; fax: +972-4-829-5672.
E-mail address: paz@tx.technion.ac.il (Y. Paz).

1010-6030/03/$ – see front matter © 2003 Published by Elsevier Science B.V.
doi:10.1016/S1010-6030(03)00224-7

[6]. Likewise, improved photosensitized H_2 evolution from water was achieved by enhancing the physical adsorption of charge-injecting dye molecules onto coated semiconductors [7]. It is noteworthy that in the above-mentioned examples, the host molecules were attached directly to the photocatalyst, hence were inherently prone to an attack by photooxidizing species that are formed on the photocatalyst.

Adsorption of contaminants in the vicinity of photocatalytic sites may increase photoefficiency. Here, the basic concept is based upon the physisorption of reactants on the inert substrates, followed by their surface-diffusion to the interface between the adsorptive sites and the photocatalytic sites. The net result is an increase in the concentration of the contaminants at the photocatalytic sites. This concentrating effect leads to an enhanced photodegradation rate, hence providing a mean to treat harmful low-level contaminants. Indeed, titanium dioxide particles partially coated with a hydrophobic organo-silicone layer [8] were found to be very efficient in the photocatalytic destruction of Permatrin [9], a water insoluble pesticide. Other examples include the photocatalytic decomposition of the herbicide propyzamide [10] by TiO_2 supported on activated carbon, the photodecomposition of pyridine over TiO_2 loaded zeolites [11], and the oxidation of nitrogen oxides [12].

Although the adsorptive approach presented above helps in promoting the photodegradation of contaminants that normally do not adsorb on the photocatalyst surface, it cannot provide a comprehensive solution to the selectivity problem, since the adsorption selectivity of the inert domains is very poor and cannot be controlled. There is a need, therefore, to extend this approach towards ways that will provide higher selectivity. One way to obtain high selectivity is to imprint [13] cavities of target molecules on the photocatalyst's surface. Within the context of selective photocatalysis, imprinting means the sol–gel polymerization of titanium dioxide around a molecule acting as a template. After polymerization, the molecular template is chemically or physically removed, to leave the imprinted molecular site. Here, a promising method was proposed by Kunitake [14], according to which a Ti(IV) alkoxide was modified by reacting with a carboxylic acid derivative of the target molecule. This method was successfully adapted recently to give high selectivity in the photodegradation of 2,4-dichlorophenoxyacetic acid [15].

A different, novel approach for obtaining high selectivity is proposed hereby. The core of this approach is the construction of robust, immobile organic molecular recognition sites (MRS) on inert domains, located on, or in the vicinity of, the photocatalyst. These molecular recognition sites are supposed to physisorb selectively the target molecules. Then, the adsorbed molecules will surface-diffuse from site to site towards the interface between the inert domains and the photocatalytic domains, where they will be destroyed (Fig. 1).

Since the molecular recognition sites are organic, care should be taken to prevent their destruction by the hydroxyl radicals formed on the titanium dioxide surface. Obviously, this means that the MRS should not be constructed directly on the photocatalytic titanium dioxide surface. Moreover, it is needed to assure that MRS located on inert sites, adjacent to photocatalytic domains are not prone to an attack by oxidizing species, diffusing from the photocatalyst domains to the inert domains. Indeed, it was found by us that such oxidizing species can destroy organic molecules anchored on oxide surfaces as far as 40 μm away from the photocatalytic domains [16], thus preventing the use of inert oxide surfaces as MRS substrates.

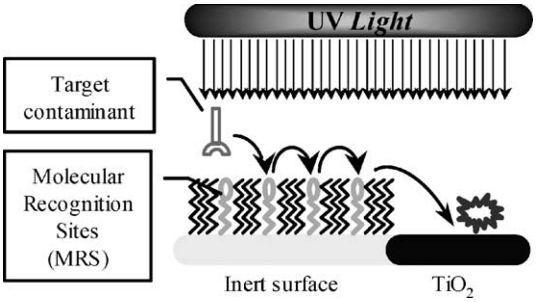

Fig. 1. The concept.

In this paper, we demonstrate the approach of mass-transport controlled selectivity by using molecules of thiolated β-cyclodextrin chemisorbed on gold as the molecular recognition sites. β-Cyclodextrin is a cyclic oligosaccharide, made of seven glucopyranose units forming a torus-like structure with a cavity of 0.78 nm in diameter. This molecule was chosen to demonstrate the mass-transport controlled photodegradation (MTCP) approach based on the well-known size-selective affinity between this molecule and a variety of apolar guests whose size matches that of the cyclodextrin cavity. Among these guest molecules are drugs, food flavors, pesticides, herbicides, and dye-stuffs [17].

Although the method is demonstrated hereby only for this host, it can easily be extended to other systems. Likewise, although the samples presented here were prepared on solid films, it should not be too complicated to extend this attitude to powders or the like.

2. Experimental

2.1. Samples' preparation

In order to demonstrate the feasibility of the mass-transport controlled photodegradation (MTCP) concept, a set of experiments was designed. This set was based upon well-defined MRS-containing micro-domains constructed on thin films of titanium dioxide on silicon wafers. Experiments were performed in five types of substrates (Fig. 2).

2.1.1. Type-I

Type-I substrates are non-patterned TiO_2-coated silicon wafers. The preparation of the type-I samples consisted

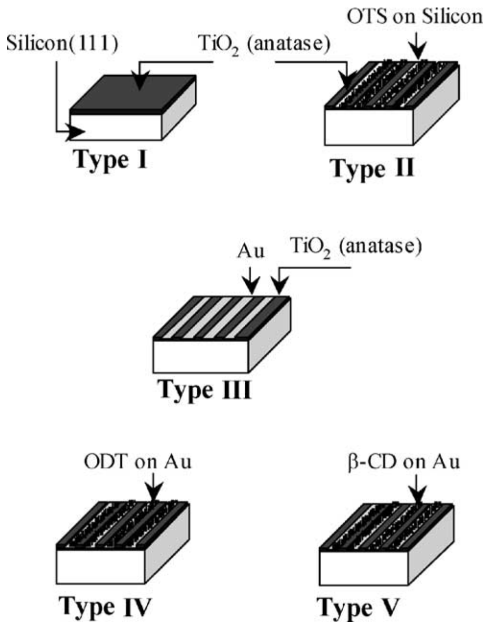

Fig. 2. The different types of hybrid structures.

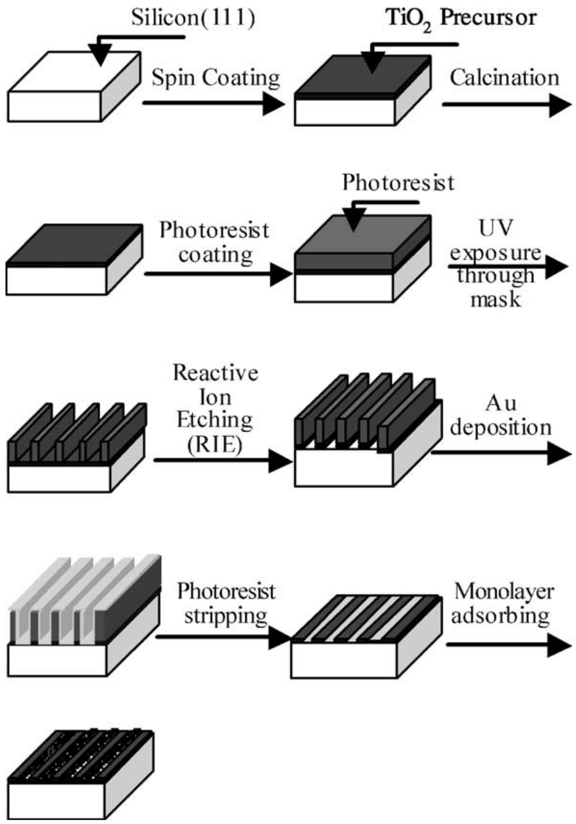

Fig. 3. Samples' preparation scheme.

of coating of a set of 1 in. silicon wafers (P-type (1 1 1), polished on both sides, 3000 Ω cm, Topsil, USA) by a thin (70 nm), well-adhered, nano-crystalline TiO_2 (anatase) film, produced by a sol–gel process, similar to the one used by us for the preparation of self-cleaning glass [18,19], but with a calcination temperature of 450 °C.

2.1.2. Type-II

Type-II samples consisted of substrates made of alternating, repeating micro-stripes of titanium dioxide and silicon, onto which self-assembled monolayers of octadecyltrichlorosilane (OTS, $CH_3(CH_2)_{17}SiCl_3$) were chemisorbed [20]. These long alkyl chains molecules are known to attach covalently to the surface of oxides by siloxane bonds, where adjacent chains are cross-linked by Si–O–Si bonds. The preparation of these samples included the following steps [21]:

- Coating of a silicon wafer with the same titanium dioxide film used for type-I samples.
- Spin-coating the TiO_2 layer with a positive photoresist (AZ1818, Shipley), then pre-baking (90 °C, 10 min).
- Exposure through a specific mask. For this stage, a set of masks, each consisting of alternating stripes of equal width and distance (40 or 80 μm) was prepared.
- Developing (DEV326, Shipley) and post-baking, leaving a structure made of protected and unprotected stripes, having predetermined width.
- Etching of the unprotected titanium dioxide domains, to the silicon substrate, by reactive ion etching (RIE), using CHF_3 plasma.
- De-scum by oxygen plasma to remove minute amounts of fluorocarbon polymers that might have formed on the etched surface during the CHF_3 RIE step.
- Photoresist stripping, followed by immersion in H_3PO_4 solution to remove any aluminum that might have been deposited during the RIE process.
- Chemisorbing OTS on the well-defined alternating stripes of titanium dioxide and (the native oxide of) the silicon stripes, using 5 mM OTS in bicyclohexyl.
- Protecting the OTS on the central part of the silicon stripes (20 μm in the 40 μm stripes, 40 μm in the 80 μm stripes) by patterned photoresist.
- Exposing the unprotected part of the samples to short UV light to photodegrade the OTS on the unprotected TiO_2 stripes.
- Stripping the photoresist from the protected silicon stripes, leaving intact the OTS monolayer on the silicon.

2.1.3. Type-III

Type-III samples consisted of alternating, repetitive micro-stripes of gold and titanium dioxide. The first step in the preparation of these samples consisted of constructing Si/TiO_2 hybrid structures (step 7 in the formation of type-II samples). Then, using a conventional lift-off process, thin metallic layers consisting of a titanium underlayers (80 Å) used as adhesion promoters and a gold top layers (750 Å thick) were deposited by evaporation and were patterned to give repetitive, alternating stripes structure of gold and titanium dioxide (Fig. 3).

2.1.4. Type-IV

Type-IV samples consisted of type-III substrates onto which self-assembled monolayers of *n*-octadecanethiol (ODT, $CH_3(CH_2)_{17}SH$) were chemisorbed from an ethanolic solution on the gold stripes (2.5–40 μm in width) but not on the titanium dioxide stripes (Fig. 3). These molecules are known to bind to metallic substrates through their thiolate groups, thus creating close packed, ordered, stable monolayers [22].

2.1.5. Type-V

Type-V samples were exactly the same as the type-IV samples except that the chemisorbed SAMs were thiolated-β-cyclodextrin (TBCD) instead of ODT. These structures were prepared by dipping type-III wafers in a DMSO/water solution (3:2 v/v), which contained 1 mM of per-6-thio-β-cyclodextrin for 12 h. A thorough washing with methanol and water, then drying under nitrogen, followed this step.

The thiolated-β-cyclodextrin used for chemisorption on the gold stripes was prepared from β-cyclodextrin (ICN Biomedicals Inc.) following the scheme of Rojas et al. [23], 11 g of triphenyl phosphine and 10.1 g of iodine were dissolved in 40 ml DMF. The reaction mixture was stirred and 2.16 g of β-cyclodextrin was added to it and the solution was refluxed at 80 °C for 15 h with constant stirring. The solution was then concentrated to half the volume by evaporation under vacuum. The pH of the solution was adjusted to 9–10 by addition of 3 M sodium methoxide in methanol and then poured in 400 ml of methanol to precipitate out iodinated β-cyclodextrin (I-CD).

0.96 g of I-CD was dissolved in 10 ml DMF and treated with 0.303 g thiourea at 70 °C for 19 h under nitrogen atmosphere ($0.8\ \mathrm{kg/cm^2}$). After that, the DMF was removed by vacuum evaporation to give viscous yellow liquid, which was dissolved in 50 ml of water. 0.26 g of sodium hydroxide was then added and the reaction mixture was heated for 1 h. The resulting suspension was acidified with aqueous $KHSO_4$ to precipitate out the thiolated β-cyclodextrin.

2.2. Substrates' characterization

All patterned structures were characterized routinely during the preparation process by optical microscopy (Olympus BX60), to assure the good quality of the pattern-transfer process. The width of the titanium dioxide domains and that of the silicon domains were measured at the end of the process by a Vickers Instrument M41 measuring system. The depth of the stripes was measured by profilometry (alpha-step 500, Tencor Inc.) at the end of the process, to assure complete etching of the titanium dioxide at the unprotected areas, and to measure the corrugation of each of the domain types. The titanium dioxide films' depth profile was characterized by argon sputtering assisted Auger spectroscopy, to assure that no other phases (such as titanium silicides) were formed at the interface between the silicon substrate and the titanium dioxide film. The same technique was used on the etched domains, to assure the completeness of the etching step and to validate the absence of contaminants on the surface, which could have formed during the RIE process.

Samples covered with self-assembled monolayers (types II, IV, V) were characterized by Fourier transformed infrared spectroscopy (Bruker IFS55, measured with $4\ \mathrm{cm^{-1}}$ resolution), either in the direct absorption mode (type-II samples) or in the reflection mode (type-IV, type-V samples).

2.3. Photodegradation measurements

The photocatalytic degradation kinetics of SAMs on inert substrates (type-II and type-IV samples) were measured inside the sample compartment of the FTIR machine, in a specially built temperature and humidity controlled accessories, which included also a UV (254 nm) pencil lamp. The illumination power at the samples' surface, as measured by a Spectroline radiometer was $0.09\ \mathrm{mW/cm^2}$.

The photodegradation kinetic measurements of contaminants on a set of type-V samples, that differed in their stripes' width, were conducted in air by exposing the samples to UV light Au/TiO_2 hybrid structures containing the adsorbed contaminants under 365 nm UV radiation ($0.07\ \mathrm{mW/cm^2}$) for different periods of time. Comparative measurements of the photodegradation of contaminants in the liquid phase using type-I, type-III, and type-V samples were performed by comparing between the disappearance rate of 2-methyl-1,4-naphthoquinone (2MNQ) versus that of benzene. Three types of solutions were prepared and measured: 2MNQ (2.3 mM), benzene (0.25 mM), and a mixture containing the two contaminants (benzene, 0.25 mM; 2MNQ, 2.3 mM). As a solvent, 60 ml of a mixture of water–propanol (1:1 v/v) was used. Experiments consisted of exposing sealed Petri dishes, containing the solutions and three identical 1 in. wafers to UV light ($0.09\ \mathrm{mW/cm^2}$) for 30 min. Aliquots were taken prior to, and after, exposure and were measured immediately by circle-cell attenuated total reflection FTIR.

3. Results and discussion

3.1. The suitability of inert micro-domains for the mass-transport controlled photodegradation (MTCP) approach

As mentioned above, the need for verifying the suitability of inert micro-domains for SRP purposes stems from the possibility that oxidizing species formed on titanium dioxide might diffuse to the inert micro-domains and might photodegrade the organic molecular recognition sites. In order to assure that any organic MRS on inert micro-domains would not be prone to such an attack, self-assembled monolayers of long alkyl chains were chemisorbed on the inert

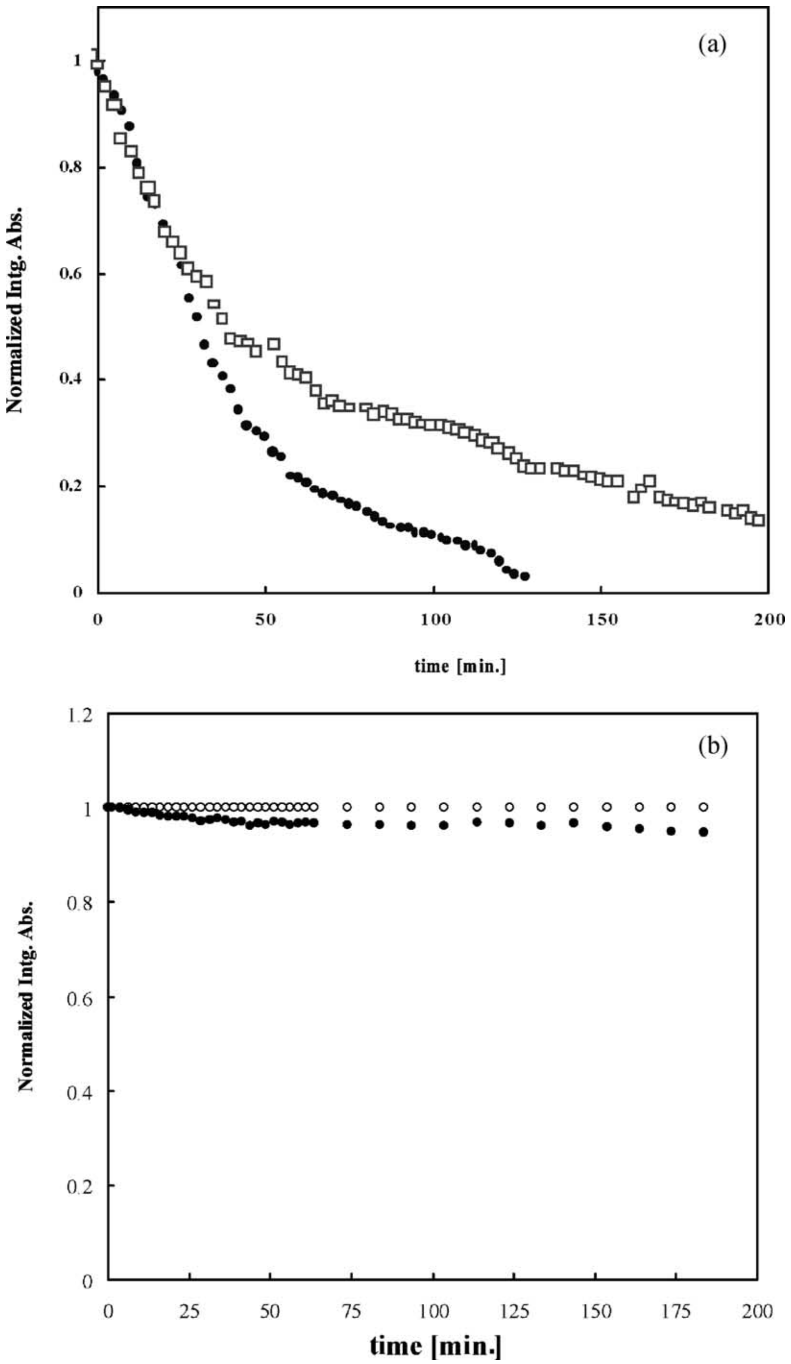

Fig. 4. (a) Changes in the normalized integrated absorbance of the C–H stretch bands of an OTS monolayer located in the middle of silicon stripes in type-II samples, due to exposure to UV light—(●) stripes' widths of TiO_2, silicon, OTS: 40, 40, 20 μm, respectively; (□) stripes' widths of TiO_2, silicon, OTS: 80, 80, 40 μm, respectively. (b) The normalized integrated absorbance of the C–H stretch bands of a monolayer of ODT on Au, in type-IV samples as a function of UV exposure time—(○) 40 μm stripes; (●) 2.5 μm stripes.

domains. The remote photodegradation kinetics of these anchored molecules was studied by following changes in the C–H stretch peaks of their spectra upon exposure to UV light. Fig. 4(a) presents the integrated absorbance of the CH stretch envelope (i.e. CH_2(a), CH_2(s), CH_3(a), CH_3(s)) as a function of exposure time for type-II samples, where 20 μm stripes of OTS were originally chemisorbed in the middle of 40 μm stripes of silicon, in a repetitive, alternating structure made of silicon and titanium dioxide stripes (40 μm in width). For clarity, results are given in a normalized manner, relative to the integrated absorption of the peaks prior to UV exposure. As demonstrated in the figure, a complete degradation could be achieved within 120 min of exposure. Under the same exposure time, a repetitive structure made of alternating titanium dioxide/silicon stripes of 80 μm in width, where the OTS molecules covered 40 μm in width of the central part of the silicon stripes lost 75% of its IR signal. The fast degradation of the OTS molecules that were anchored on the silicon micro-stripes evidently shows that this configuration of silicon substrate and an alkyl chain attached to the surface by siloxane bonds is inadequate for constructing stable molecular recognition sites that will act to trap and shuttle contaminants of interest.

This instability towards remote degradation was not found when a self-assembled monolayer anchored through a thiol functional group to metallic stripes was examined. Fig. 4(b) shows changes in the normalized integrated absorbance of the CH stretch envelope in the spectra of ODT that was chemisorbed on type-IV samples upon exposure to UV light. Results are given for a repetitive structure made of 40 μm in width titanium dioxide stripes and 40 μm in width gold stripes (empty circles) and for a repetitive structure made of 2.5 μm in width titanium dioxide stripes and 2.5 μm in width gold stripes (filled circles). Regardless of the width of the stripes, and despite the fact that the required diffusion distance in the type-IV samples was smaller than in the type-II samples, hardly any degradation could be observed in the monolayer anchored on the gold substrates. The same stability towards remote photodegradation was observed even when the illumination flux was increased by one order of magnitude, or when the ODT monolayer was chemisorbed on platinum.

In order to clarify this observed difference between ODT on gold and OTS on silicon, another set of measurements was performed with OTS chemisorbed on the native oxide of aluminum. The preparation of these samples was similar to that of type-IV samples, except for the chemisorption of OTS instead of ODT. Here, under the same conditions, complete photodegradation required 200 min for 2.5 μm in width stripes and approximately 420 min for structures made of stripes having 40 μm in width. Since ODT and OTS are both long alkyl chains that differ only in the functional groups that attach them to the surface, it is likely that the main factor determining whether remote degradation might occur was not the type of self-assembled monolayer but rather the type of inorganic substrate. Published work on the room temperature reaction between OH$^{\bullet}$ radicals and these three types of inorganic surfaces [24] reveals that gold is the most reactive among these three surfaces; the reaction probability of hydroxyl radicals with silicon dioxide was found to be only 2×10^{-3}, with alumina 5×10^{-3} and with gold as large as 3×10^{-2}. The stability of SAMs on gold is then explained by the reaction between the gold and hydroxyl radicals that reduces the number of hydroxyl radicals available for attacking the organic monolayer.

3.2. Demonstrating the MTCP concept, using thiolated β-cyclodextrin as molecular recognition sites

The observation that molecules attached to gold domains located at the vicinity of titanium dioxide do not degrade upon exposure of the photocatalyst surface to UV light paves the way for constructing molecular recognition sites on gold micro-domains that would serve to physisorb molecules of interest, later to be shuttled to the photocatalytic sites.

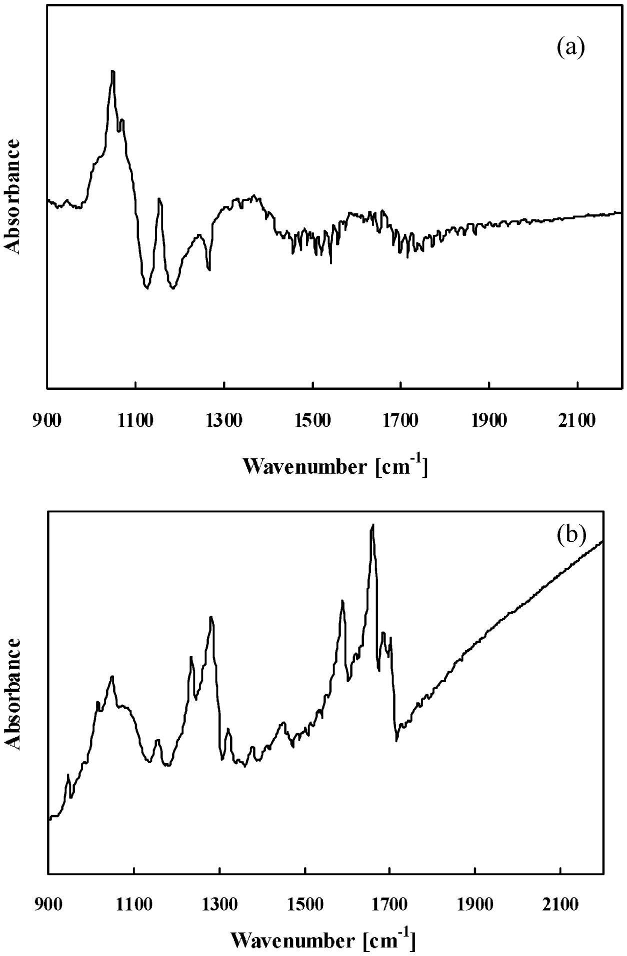

Fig. 5. (a) FTIR spectrum of thiolated cyclodextrin chemisorbed on gold, (b) FTIR spectrum of 2MNQ on a monolayer of thiolated cyclodextrin.

As mentioned earlier, β-cyclodextrin was chosen as the first host to demonstrate the MTCP concept, due to its high well-documented ability to form inclusion complexes with a variety of potential contaminants. In order to chemisorb it to gold micro-domains, care had to be taken to thiolate this host, as described in the experimental section. Fig. 5(a) presents the reflection mode FTIR spectrum of a type-V sample. The spectrum is similar to the one reported by Nelles et al. [25] where coupled ν(C–C/C–O) vibrations at 1048 and 1069 cm^{-1} and a prominent absorption peak at 1157 cm^{-1}, corresponding to the antisymmetric (C–O–C) stretching vibration, were observed.

In order to validate that the molecular recognition sites constructed in the vicinity of photocatalytic micro-domains are capable to host and shuttle contaminants of interest, 2-methyl-1,4-naphthoquinone was used. Fig. 5(b) shows the reflectance mode spectrum taken after immersion in a 2 mM solution of 2-methyl-1,4-naphthoquinone (2MNQ) in water–propanol (1:1 v:v) for 12 h, followed by thorough

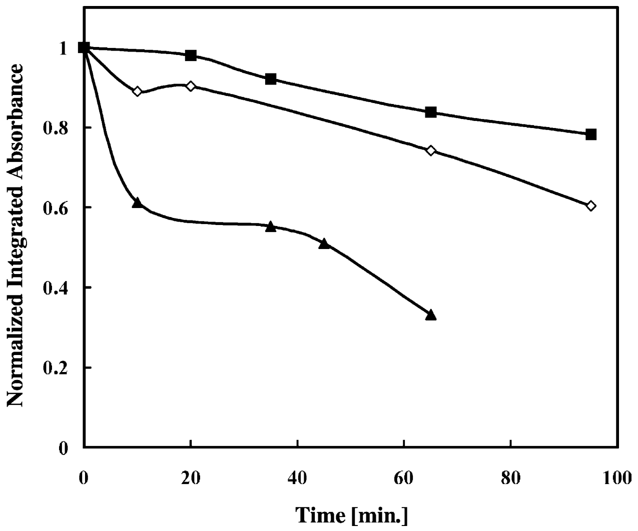

Fig. 6. The photodegradation kinetics of 2-methylnaphthoquinone on the type-V wafers for samples containing Au/TiO_2 stripes of different width. In all samples, the width of the gold stripes was equal to that of the TiO_2 stripes. Filled triangles represent stripes of 5 μm in width, empty diamonds represent stripes of 20 μm in width, and filled squares represent stripes of 40 μm in width.

washing and drying. The spectrum reveals typical naphthoquinone peaks at 1666 and 1594 cm^{-1}, together with a slight shifting in the 1157 cm^{-1} cyclodextrin-related peak to 1154 cm^{-1}, most likely reflecting the formation of the cyclodextrin–naphthoquinone inclusion complex. No evidence for 2MNQ adsorption neither on gold nor on TiO_2 was found when type-I or type-III samples were immersed in the same manner, and measured by both reflection and direct absorption modes.

Fig. 6 presents the kinetics of photocatalytic degradation of 2MNQ physisorbed on the thiolated cyclodextrin, as deduced from the reduction in the area of the 1666 cm^{-1} peak, for structures having stripes of different sizes. As usual, the width of the gold stripes in all wafers was equal to that of the titanium dioxide, such that the photocatalytic area was equal to 50% of the total area of the wafers. As shown in the figure, the smaller the domain width was, the faster the photodegradation of the 2-methyl-1,4-naphthoquinone was. For example, 20% degradation was obtained with the 5 μm width structure after 5 min, whereas the same extent of degradation with the 40 μm width structure required 90 min. This effect of the domain size is in line with the notion that the 2MNQ molecules were adsorbed on the molecular recognition sites, from where they had to diffuse to the photocatalytic titanium dioxide domains. This conclusion is supported by the observation that the degradation of the 2MNQ was not accompanied by the degradation of the molecular recognition sites, since otherwise the degradation of the MRS would have been observed. To assure that the degradation was not due to direct photolysis, or to the presence of gold per se, a control experiment, where 2MNQ adsorbed on β-cyclodextrin chemisorbed on gold-coated silicon (without titanium dioxide) was held. In this case, the amount of 2MNQ on the surface remained the same even after 1 h of exposure.

A comparative study on the ability of the type-V structures to enhance the degradation of selected contaminants was done in the liquid phase by comparing between the rate of disappearance of 2MNQ versus that of benzene. The measurements were performed with type-III and type-V samples (both having stripes' width of 5 μm), as well as with type-I wafers. Table 1 presents the extent of decrease in the concentration of both contaminants following 30 min of exposure, and the ratio between the relative degradation in 2MNQ to that of benzene, for solutions containing one contaminant at a time and for solutions containing both contaminants at the same time. A comparison between the three types of wafers reveals that for both types of solutions the type-V wafers were significantly more efficient in photodegrading 2MNQ than the type-III wafers (60% degradation versus 18.7% degradation, i.e. more than 200% faster), demonstrating the enhancement in photodegradation due to the molecular recognition sites. In contrast, the photodegradation rate for benzene with the type-V wafers was lower than that with the type-III wafers. The overall effect is reflected in the ratio between the degradation rate of 2MNQ to that of benzene, where an increase of more than 10 times (8.1:0.75) was found when comparing solutions containing one contaminant at a time, and an increase of six times (4.2:0.71) when solutions containing a mixture of the two contaminants were compared. Hence, the feasibility of enhancing the preferential degradation of selected contaminants by constructing molecular recognition sites at the vicinity of titanium dioxide domains was clearly demonstrated.

Both 2MNQ and benzene are known to form inclusion complexes with β-cyclodextrin [26,27]. The negative effect measured with benzene can be explained by very low surface mobility of benzene, probably due to high complexing energy between the host and the guest. Such an explanation

Table 1
The extent of decrease in the concentration of benzene and of 2-methylnaphthoquinone, following exposure of vessels containing the various types of wafers to 365 nm light, and the ratio between the extent of degradation of 2MNQ to that of benzene

	One contaminant solutions			Two contaminants solutions		
	Type-I (TiO_2)	Type-III (Au/TiO_2)	Type-V (CD/Au/TiO_2)	Type-I (TiO_2)	Type-III (Au/TiO_2)	Type-V (CD/Au/TiO_2)
2MNQ (%)	22.3	18.7	60	13	19.8	32.6
Benzene (%)	26	25	7.4	26.3	28	7.7
2MNQ/benzene	0.86	0.75	8.11	0.49	0.71	4.23

goes well with the notion that benzene penetrates very deep into the cavity of β-cyclodextrin, forming a very tight 1:1 complex [28].

Another model contaminant that shows enhanced rate of photodegradation due to the presence of β-cyclodextrin close to titanium dioxide micro-domains is the dye-stuff Chicago Blue Sky 6 (CB). Here, an aqueous solution containing a mixture of 0.01 mM of Chicago Blue and 0.01 mM of the dye-stuff Rhodamine 6G was exposed to 365 nm UV light (0.09 mW/cm^2), in the presence of either three wafers of type-III samples or three type-V wafers. The degradation of the Chicago Blue dye and that of R6G was calculated based on changes in their UV-Vis spectra, as reflected in their 625 and 527 nm peaks, respectively. It was found that the degradation of the Chicago blue was 1.7 times (70%) faster when using the type-V samples than when using the type-III samples. This enhancement was not observed for R6G. It is suggested, albeit not proved, that the enhancement in the photodegradation of Chicago Blue is closely related with its structure. The CB molecule is a long, symmetric molecule, made of two "hands". Each "hand" consists of two conjugated aromatic rings, substituted with two SO_3Na moieties. The "hands" are connected through N=N bridge to another substituted aromatic ring, which is connected to the other "hand". The cavity of β-cyclodextrin can accommodate no more than one substituted ring, hence only a small part of the molecule is attached inside the cavity, while most of the long residue is out of the cavity, and may physisorb on a second β-CD molecule. As said before, the movement towards the titanium dioxide interface may require the contaminants to have sufficient energy to overcome the host–guest interaction, otherwise the guest molecules would stick in the cavity of the hosts. At the same time, too much energy might cause desorption. An interesting question would be whether the symmetrical structure of the CB, which allows for two anchors with the surface, helps in stabilizing the molecule on the surface without introducing effective limitations on its surface-diffusion.

4. Conclusions

A new approach for enhancing the photocatalytic degradation of specific contaminants in air or water is presented herein. The method is based upon selective physisorption of the contaminants in the vicinity of titanium dioxide micro-domains, followed by surface-diffusion of the contaminants to the photocatalytic sites. The feasibility of this approach is demonstrated while using β-cyclodextrin as a host and 2-methyl-1,4-naphthoquinone and the dye-stuff Chicago Blue as guests. Results also point to the fact that such an enhancement requires a delicate balance between adsorption, desorption, and surface-diffusion.

Since both adsorption, desorption and diffusion are temperature dependent phenomena, it is likely that changing the temperature may alter the enhancement factor. Moreover, the above-described effects are expected to be more pronounced with smaller domains, where the diffusion length is shorter. Work along these lines, with other systems and with powders, is currently underway and will be presented elsewhere.

Acknowledgements

This work was funded by the Israeli Ministry of Science and by the 5th framework of the European Commission. The support of the Water Research Institute at the Technion is also acknowledged.

References

[1] (a) M.M. Holmann, Photodegradation of Water Pollutants, CRC Press, Boca Raton, FL, 1996;
(b) D.M. Blake, Bibliography of Work on the Photocatalytic Removal of Hazardous Compounds from Water and Air, NREL, Golden, CO, 1999;
(c) A. Mills, S.J. Le Hunte, Photochem. Photobiol. A 108 (1997) 1;
(d) A. Fujishima, K. Hashimoto, T. Watanabe, TiO_2 Photocatalysis, BKC, Tokyo, 1999;
(e) D.F. Ollis, Catal. Tech. 2 (1998) 149;
(f) M.I. Litter, Appl. Catal. B 23 (1999) 89.

[2] R.W. Matthews, Water Res. 20 (1986) 569.

[3] M.A. Fox, M.T. Dulay, Chem. Rev. 93 (1993) 341.

[4] P. Salvador, J. Electrochem. Soc. 128 (1981) 1895.

[5] J. Chen, D.F. Ollis, W.H. Rulkens, H. Bruning, Water Res. 33 (1999) 661.

[6] T. Rajh, O. Makarova, M.C. Thurnauer, P.A. Kemme, D. Cropek, Proceedings of the 222nd ACS Meeting, Chicago, IL, 2001.

[7] I. Willner, Y. Eichen, J. Am. Chem. Soc. 111 (1989) 1884.

[8] G. Dagan, S. Sampath, O. Lev, Chem. Mater. 7 (1995) 446.

[9] H. Hidaka, K. Nohara, J. Zhao, N. Serpone, E. Pelizzetti, J. Photochem. Photobiol. A 64 (1992) 247.

[10] H. Uchida, S. Itoh, H. Yoneyama, Chem. Lett. 1995 (1993).

[11] S. Sampath, H. Uchida, H. Yoneyama, J. Catal. 149 (1994) 189.

[12] T. Ibusuki, K. Takeuchi, J. Mol. Catal. 88 (1994) 93.

[13] (a) G. Wulff, Angew. Chem., Int. Ed. Engl. 34 (1995) 1812;
(b) O. Ramstörm, R.J. Ansell, Chirality 10 (1998) 195;
(c) K. Mosbach, Trends Biochem. Sci. 19 (1994) 9;
(d) K.J. Shea, Trends Polym. Sci. 2 (1994) 166;
(e) G. Wulff, in: J. Siegel (Ed.), Supramolecular Chemistry, Kluwer Academic Publishers, Dordrecht, The Netherlands, 1995;
(f) K. Haupt, K. Mosbach, Trends Biotechnol. 16 (1998) 468;
(g) S. Rimmer, Chromatographia 47 (1998) 470;
(h) B. Sellergren, ACS Symp. Ser. 703 (1998) 49–80.

[14] (a) S.-W. Lee, I. Ichinose, T. Kunitake, Langmuir 14 (1998) 2857;
(b) S.-W. Lee, I. Ichinose, T. Kunitake, Chem. Lett. 1193 (1998);
(c) I. Ichinose, H. Senzu, T. Kunitake, Chem. Lett. 831 (1996);
(d) I. Ichinose, T. Kawakami, T. Kunitake, Adv. Mater. 10 (1998) 535;
(e) Y. Lvov, K. Ariga, I. Ichinose, T. Kunitake, J. Am. Chem. Soc. 117 (1995) 6117.

[15] I. Willner, Unpublished results.

[16] H. Haick, Y. Paz, J. Phys. Chem. B 105 (2001) 3045.

[17] (a) J. Szejtli, Cyclodextrin Technology, Kluwer Academic Publishers, Dordrecht, The Netherlands, 1988;
(b) K.A. Connors, Chem. Rev. 97 (1997) 1325.

[18] Y. Paz, Z. Luo, L. Rabenberg, A. Heller, J. Mater. Res. 10 (1995) 2842.

[19] Y. Paz, A. Heller, J. Mater. Res. 12 (1997) 2759.

[20] J. Sagiv, J. Am. Chem. Soc. 102 (1980) 92.
[21] E. Zemel, H. Haick, Y. Paz, J. Adv. Oxid. Technol. 5 (2002) 27.
[22] A. Ulman, An Introduction to Ultrathin Organic Films, Academic Press, London, 1991.
[23] M.T. Rojas, R. Königer, J. Fraser Stoddart, A.E. Kaifer, J. Am. Chem. Soc. 117 (1995) 336.
[24] M. Suh, P.S. Bagus, S. Pak, M.P. Rosynek, J.H. Lunsford, J. Phys. Chem. B 104 (2000) 2736.
[25] G. Nelles, M. Weisser, R. Back, P. Wohlfart, G. Wenz, S. Mittler-Neher, J. Am. Chem. Soc. 118 (1996) 5039.
[26] L. Pang, M.A. Whitehead, Supramol. Chem. 1 (1992) 81.
[27] J.Y. Lee, S. Park, J. Phys. Chem. B 102 (1998) 9940.
[28] E.E. Tucker, S.D. Christian, J. Am. Chem. Soc. 106 (1984) 1942.